Macromol. Symp. 2008, 261, 85–90 DOI: 10.1002/masy.200850111

Characterization of Polymer Architectures by Multidetection Size Exclusion Chromatography

Judit E. Puskas, Elizabeth A. Foreman, Lucas M. Dos Santos, Serap Hayat Soytaş*

Summary: This paper discusses the analysis of star-branched and dendritic polyisobutylenes (PIBs) using branching parameters based on radii of gyration $R_{g,z}$ and hydrodynamic radii $R_{h,z}$. $R_{g,z}$ and $R_{h,z}$ were measured by Size Exclusion Chromatography equipped with a Wyatt Technology Viscostar viscometer (VIS), a Wyatt Optilab DSP RI detector, a Wyatt DAWN EOS 18 angle Multiangle Light Scattering (MALS) detector and a Wyatt Quasi-elastic Light Scattering QELS detector. Branching parameters were calculated from these measurements and compared with those computed for these architectures.

Keywords: arborescent; dendritic; living carbocationic polyisobutylene; multidetector SEC; polymerization; star-branched

Introduction

Branched polymers have attracted much attention, due to their distinct and unique physical properties both in solution and in solid state, in comparison with their linear counterparts. Macromolecular engineering using various living/controlled polymerization techniques is the most versatile technique to synthesize various polymeric architectures.[1] There has also been a great deal of interest to investigate structure-property relationships in these architectures. Polyisobutylene (PIB) is an ideal model polymer for structure-property relationship studies; because due to its chemical structure it has excellent chemical and heat stability, allowing rheological investigations in a wide temperature range.[2] We have developed living carbocationic polymerizations that produce high molecular weight (MW) arborescent (dendritic) and star-branched PIBs shown in Figure 1 and 2 respectively.[3–6]

Burchard, Schmidt and Stockmayer discussed the analysis of various polymer architectures based on R_g amd R_h data (radius of gyration and hydrodynamic radius, respectively.[6] They computed these parameters for mono- and polydisperse linear and star-branched model polymers with *f* number of arms (‘‘rays’’), ‘‘random polycondensates’’ (hyperbranched structures) of A_f or ABC type (identical or different functional groups, respectively) and randomly branched/crosslinked polymers. From this they identified the parameters *g*, *h* and *ρ* which gave insight into polymer architectures.

$$g = \left(\frac{\left\langle R_g^2\right\rangle_{br}}{\left\langle R_g^2\right\rangle_{lin}}\right)_{M_w}$$

$$h = \left(\frac{D_{lin}}{D_{br}}\right)_{M_W} = \left(\frac{R_h br}{R_h lin}\right)_{M_W} \qquad (1)$$

$$\rho = \left(\frac{\left\langle R_g^2\right\rangle^{1/2}}{R_{h,z}}\right)$$

Equation 1 show these parameters where $\langle R^2\rangle_{\mathrm{br}}$ and $\langle R^2\rangle_{\mathrm{lin}}$ are the mean-square radii of branched and linear polymers of the same weight-average molecular weight, and $R_{h,z}$ is the effective z-average Stokes-Einstein hydrodynamic radius. Burchard et al.[6] wrote ‘‘It is commonly

---

Department of Polymer Science, The University of Akron, 170 University Av. Akron, OH 44325-3909, USA
Fax: (001)-330-972-5290;
E-mail: jpuskas@uakron.edu

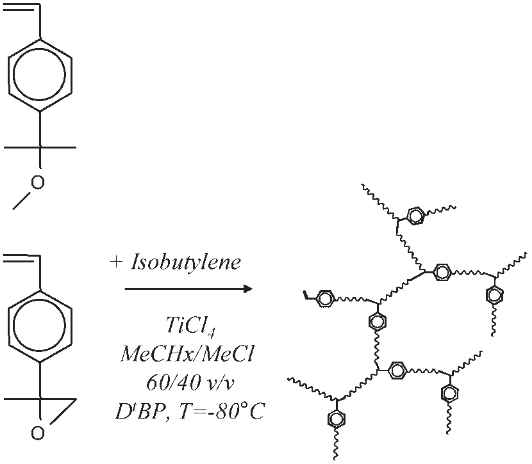

Figure 1.
Synthesis of *arb*PIBs by inimer-type living carbocationic polymerization.[3,4]

presumed that *g* and *h* are continuously decreasing functions of the branching density and always smaller than unity. This statement is certainly correct for monodisperse samples and also holds for regular stars. In the other cases, however, *g* and *h* are larger than unity for low branching densities, and in the case of randomly branched polycondensates or randomly cross-linked molecules they even *increase* with the number of functional groups, in contrast to the decrease for star molecules. The reason for this behavior is that polydispersity causes a larger increase of the z-average mean-square radius of gyration than the corresponding increase of the weight-average molecular weight. Thus *g* and *h* embody two effects with converse behavior: polydispersity, which causes an increase, and branching, which causes the familiar decrease." The authors found striking similarities between the scattering behavior of linear chains with the most probable distribution ($M_w/M_n \sim 2$), and A_f type "polycondensates". They explained this with the most probable distribution of the branch lengths in these latter architectures. This does not hold for monodisperse linear and star molecules and ABC polycondensates. The formulas for polydisperse stars and "ABC polycondensates" give identical results with B = (f-1)/2 where B is the average number of branching points in the randomly branched structures, except that *f* is constant across the distribution in stars while B is increasing with MW in the randomly branched polymers.

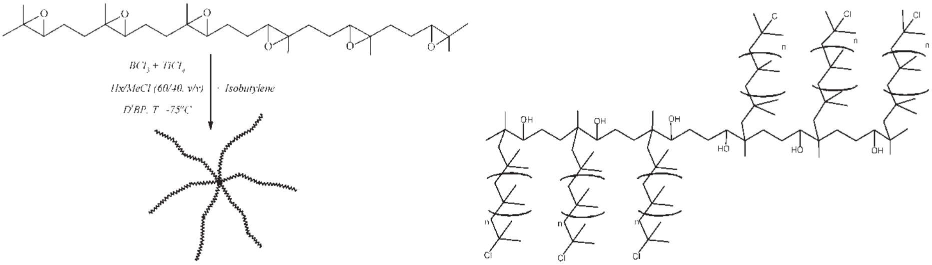

Figure 2.
Synthesis of star-branched PIB by living carbocationic polymerization.[5]

Thus, *g, h* and ρ are parameters which can give us insight into polymer architectures. Unfortunately, *g* and *h* are difficult to obtain experimentally, mostly due to the unavailability of monodisperse linear standards. In contrast, ρ can readily be obtained from $\langle R^2\rangle$ directly measured from the angle dependence of LS and D_z measured by QELS (Equation 2).

$$D_z = \frac{k_B \cdot T}{6 \cdot \pi \cdot \eta_0}\left\langle\frac{1}{R_h}\right\rangle_z \tag{2}$$

The authors emphasized that ρ is a function of branching, polydispersity and branch flexibility, but independent of bond angles and the degree of polymerization. Therefore this parameter was marked as the most reliable and accurate to give information on polymer architecture. In the single comparative example given, measured ρ values for poly(vinyl acetate) made by emulsion polymerization (PVAc) were compared with those computed for the model structures. At lower conversion/molecular weight $\rho = 1.84$ was found, only slightly higher than the theoretically expected $\rho = 1.73$ for a randomly branched architecture. ρ slightly decreased with increasing MW, indicating that branching was not completely random. Above MW $\sim 15 \times 10^6$ g/mol, ρ dropped sharply to 0.55, which is consistent with a more compact spherical shape. The authors also pointed out that $g > 2$ and $h > 1$ would clearly indicate random branching.

This paper will discuss the analysis of various PIB architectures using multidetection Size Exclusion Chromatography (SEC).

Experimental Part

PIBs were synthesized as reported[3–5] and analyzed with a Waters setup equipped with 6 Styragel columns (HR0.5, HR1, HR3, HR4, HR5, and HR6) thermostated at 35 °C, a Wyatt Technology Viscostar viscometer (VIS), a Wyatt Optilab DSP refractive index (RI) detector thermostatted at 40 °C, a Wyatt DAWN EOS 18 angle Multiangle Light Scattering (MALS) detector, a Wyatt Quasi-elastic Light Scattering (QELS) detector and a Waters 2487 Dual Absorbance UV detector. THF freshly distilled from CaH_2 was used as the mobile phase at a flow rate of 1 mL/min. Absolute molecular weights, radii of gyration and hydrodynamic radii were determined using ASTRA® V software version 5.1.6.0, with $dn/dc = 0.108$ for PIB, or assuming 100% recovery on the columns.

Results and Discussion

The z-average *g, h* and ρ data obtainable by SEC corresponds to the batch data of Stockmayer et al.[6] First we investigated the accuracy and precision of $R_{h,z}$ measurements using linear PSt and PIB standards by VIS and QELS. We found that there was good agreement between average values measured by these two methods, but viscometry was more precise and reproducible. The $R_{g,z}$ of the branched PIBs were measured by MALS from the angle dependence of light scattering, and *g* was then calculated using $R_{g,z}$ data generated with linear PIB standards, normalized by MWD.[5] $R_{h,z}$ was obtained using the viscometer on-line, and ρ was calculated as $R_{g,z}/R_{h,z}$. The ASTRA® V software also computes B using Equation 3 comparing R_g data generated with linear PIB standards, taking the actual R_g measured for the nearly monodisperse slice at the same MW as that of the branched polymer.

$$g = \frac{6}{B}\left\{\frac{1}{2}\left(\frac{2+B}{B}\right)^{1/2}\ln\left[\frac{(2+B)^{1/2}+B^{1/2}}{(2+B)^{1/2}-B^{1/2}}\right]-1\right\} \tag{3}$$

Table 1 shows data for star-branched PIBs from the hexafunctional hexaepoxysqualene (HES) initiator (more synthesis details will be published shortly), and *arb*PIBs from the 4-(2-methoxyisopropyl) styrene inimer (MeOIM) and the 4-(1,2-oxirane-isopropyl) styrene inimer (EPOIM).[3,4]

The $g = 0.74$ obtained for the HES-initiated star PIB is close to that predicted

Table 1.
SEC analysis of PIBs.

Sample ID	M_n kg/mol	M_w/M_n	η_w dl/g	$R_{h,z}$ nm	$R_{g,z}$ nm	g	h	ρ	g'	f
SH061307-4	63.2	1.27	38.2	8.7	8.8	0.74	1.04	1.01	0.90	6
06DNX040-1	57.0	1.53	34.3	9.9	16.3	2.33	1.17	1.65	0.86	4
06DNX040-2	116.6	1.49	50.7	14.2	24.2	2.46	1.14	1.70	0.74	4
05DNX190-1	123.7	1.47	54.6	14.0	17.7	1.25	1.10	1.26	0.80	4
06DNX110-3	80.1	1.33	40.5	10.7	19.3	2.61	1.13	1.80	0.83	4
06DNX110-4	114.4	1.39	64.4	17.2	24.3	1.63	1.11	1.41	0.71	4
06DNX120-3	71.7	1.33	37.4	10.2	20.4	3.31	1.15	2.00	0.84	3
06DNX120-5	115.7	1.40	50.8	12.9	18.8	1.60	1.08	1.46	0.78	3

for a six-arm polydisperse star.[6] g' shows little viscosity decrease, most likely due to the relatively short arms (the entanglement MW of PIB is $M_e \sim 10{,}000$ g/mol). The B distribution (B vs MW) from ASTRA® V was independent of molecular weight, as expected from star polymers with $B = 1$.

The architecture of *arb*PIBs arising from inimer-type living polymerization resembles one branched cluster of a dendrimer, with longer chains between fewer branch points. In terms of Burchard's models, we can compare them with crosslinked polymers except that the three-functional *inimers* lead to branching without gelation. The molecular weight distribution (MWD) of these polymers is broad with multimodal, since fractions with more living branches grow faster and produce higher MW fractions. B_{kin}, the kinetic average number of branches per chain, was calculated assuming random branching, i.e., similar reactivities of the initiating and vinyl sites of the inimer, and the growing active sites using Equation 4, where $M_{n,theo}$ stands for the MW that would arise if the *inimer* would only act as initiator and is calculated using Equation 5.

$$B_{kin} = \left(\frac{M_{n,total}}{M_{n,theo}}\right) - 1 \tag{4}$$

$$M_{n\,theo} = \frac{IB(\mathrm{g})}{IM\,(\mathrm{moles})} \tag{5}$$

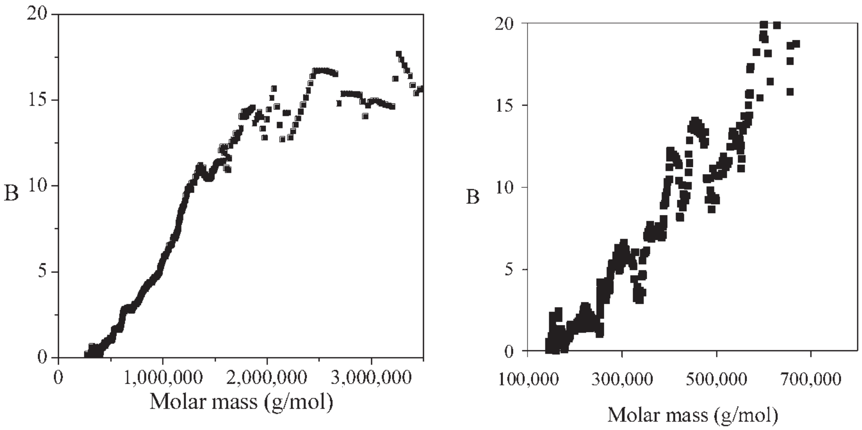

(a) 06DNX040-4 (b) 06DNX120-5

Figure 3.
Branching plots from ASTRA® V for (a) MeOIM (b) EPOIM edit figure.

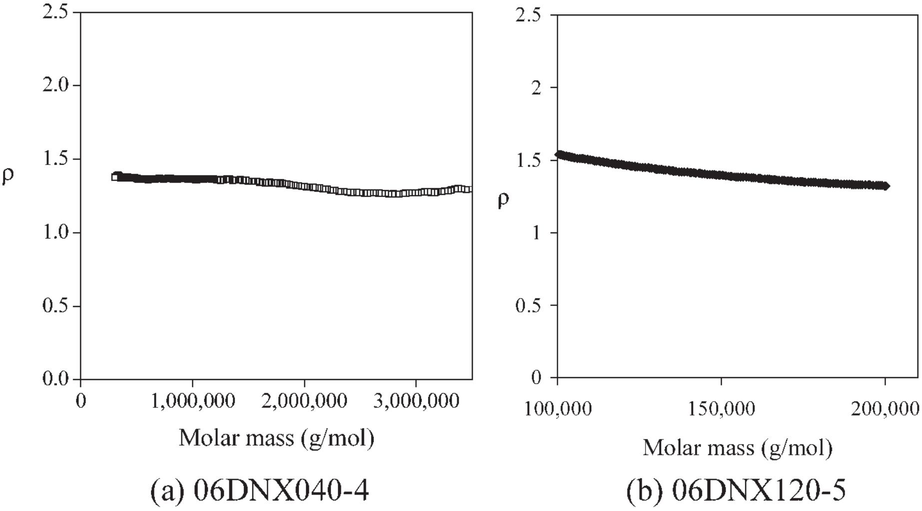

(a) 06DNX040-4

(b) 06DNX120-5

Figure 4.
ρ distribution in MeOIM (a) and EPOIM (b) initiated *arb*PIBs.

In these structures, the average number of chain ends is $f = B + 2$. The low average f values show slightly branched structures, with large $R_{g,z}$ values. Several samples have $g > 2$, $h > 1.1$ and ρ close to the 1.73 theoretically predicted for randomly branched systems.[5]

$1 < g < 2$, $h > 1$ and $\rho < 1.73$ indicate less than random branching. Table 1 also lists $g' = [\eta]_{w,br}/[\eta]_{w,lin}$ values, showing the expected reduction with increasing branching. In all dendritic samples B increased with MW across the molecular weight distribution up to about 16–20 which can be seen in Figure 3 below.

Figure 4 shows the ρ distribution for MeOIM (a) and EPOIM (b) initiated polymerizations; R_g and R_h given for each SEC fraction by ASTRA were used for these calculations. In the case of self-similar dendritic architectures constant R_g/R_h ratio is expected. Indeed, ρ remained constant across the whole molecular weight distribution in the former, while somewhat decreased in the latter.

We have found that the dendritic architecture increases the entropic contribution in the phase transition of *arb*PIB-based block copolymers, leading to unique properties.[9] Characterization of these polymers continues in our lab.

Conclusions

Multidetection SEC analysis is a very useful tool in the analysis of polymer architectures. We have shown in this paper that comparison of parameters obtained from $R_{g,z}$ and $R_{h,z}$ values computed by Burchard et al. for star and randomly branched architectures, with measured values give insight which could be useful in better understanding of structure-property relationships. Multidetection SEC was also useful to see the distribution of branching parameters across the molecular weight distribution.

Acknowledgements: This material is based upon work supported by the National Science Foundation under DMR-0509687. Financial support by LANXESS Inc. is also acknowledged. The authors would like to thank Dr. Gabor Kaszas for his contribution to this work.

[1] Macromolecular Engineering, K. Matyjaszewski, Y. Gnanou, L. Leibler, Eds., Wiley-VCH, **2007**.

[2] J. E. Puskas, P. Antony, Y. Kwon, C. Paulo, M. Kovar, P. R. Norton, G. Kaszas, V. Alstädt, *Macromol. Mater. Eng.* **2001**, *286*, 565.
[3] C. Paulo, J. E. Puskas, *Macromolecules* **2001**, *34*, 734.
[4] E. A. Foreman, J. E. Puskas, G. Kaszas, *J. Polym. Sci. A.* **2007**, in press.
[5] S. Hayat Soytaş, J. E. Puskas, K. Kulbaba, **2007**, Proceedings of CLP07, October25–29, Antalya, Turkey, 13.
[6] W. Burchard, M. Schmidt, W. H. Stockmayer, *Macromolecules* **1980**, *13*, 1265.
[7] P. J. Flory, *J. Am. Chem. Soc.* **1941**, *63*, 3083.
[8] D. A. Tomalia, H. Baker, J. Dewald, M. Hall, G. Kallos, S. Martin, J. Roeck, J. Ryder, P. Smith, *Macromolecules* **1986**, *19*, 2466.
[9] J. E. Puskas, L. Dos Santos, G. Kaszas, *J. Polym. Sci. A.* **2006**, *44*, 6494.